TS-SSC-91-32

PERIODIC REMNANT FIELD IN SSC 50mm DIPOLE

M.Wake, T.S.Jaffery and M.J.Lamm
Fermilab, PO.Box 500, Batavia IL 60510 U.S.A.
(February 15, 1991)

Introduction

Recent field measurements in HERA dipole magnets uncovered a longitudinal periodic pattern of sextupole moment which was not expected from the geometry of the magnet[1]. Although the direct effect of the periodicity would not be very large to the performance of the accelerator, the curious behavior of this pattern need to be understood to control the time dependence of the field quality which might be a large problem for the injection of the beam.

During the excitation test of the first short 50 mm dipole magnet (DSA321), we have tried to measure the remnant field distribution using Rawson-Lush type 789 field meter which is a quarter-inch rotating coil of high precision.

As a result, we observed a clear periodic pattern of magnetic field. The characteristics of the pattern was basically similar to what was observed in the sextupole moment measurement at DESY. Although, there is somewhat different information in the data obtained. The discussion on the cause of the phenomena is made together with the presentation of the data.

Experimental

In the excitation test environment, the magnet DSA321 was hanged vertically in a cryostat. A warm bore was inserted in the bore of the magnet. A Rawson-Lush type 789 field meter with vacuum insulated jacket was inserted in the warm bore. The probe was moved up and down using gear mechanism by hand. A simple position sensor made of helipot is used to find the vertical position of the probe. The center of the measurement coil is roughly guided to the horizontal center of the warm bore by the physical size of the probe. The analog output of the Rawson-Lush field meter was read into a computer through DVM. After the magnet was quenched, data were taken in successive, at the following current: 50, 100, 200, 400 on upward, 100 and

0 on the downward.The data were taken in various occasions in the course of the usual test procedure of the dipole magnet. Therefore the absolute value of some data may have a little differnt offset error.

Results

Figure 1 is the measurement results of the field with transport current which surely shows that the periodic field is a phenomena which is related with the hysteresis of the superconductor. The x-axis has its origin at the center of the magnet. The y-axis is the field subtracted by the linear field due to the current. The data were taken starting after a quench increasing current as at 50 A, 100 A, 200 A, 400 A and in the down ward at 100 A and 0 A. The bump at the negative side of the center is the effect of the pressure gage beam[2]. SSC short magnet has a set of pressure gage to measure the preloading of the coils at this position. The beam used to find the pressure from it's bending has a small magnetization at low temperature. The growth of this bump with the increased current indicates the sensitivity of this measurement.

The periodic pattern in the field was not observed just after a quench or when it had a current. But the remnant field after the current is removed showed a periodic pattern even when the ramp was only up to 400 A. Although the scale of Figure 1. is not adequate to see the pattern, there is a clear pattern in the signal. Enlarged view is shown in Fig.2.

Figure 2 is the periodic patterns after ramps with different maximum currents. The sweep rate of the ramp in the 1000 A ramp and 7000 A ramp were both 100 A/sec. The amplitude of the periodic field became larger when it was excited to the higher field but the phase of the signal stayed the same.

Since the amplitude of the periodic field is reported to have a dependency on the number of ramps the magnet had experienced after a quench, we also tried to observe it. Figure 3 is the result of the measurements. There was no significant change in those signals. The ramp rate was 100 A/sec and the magnet stayed at 7000 A for 1 minutes in every ramp.

The wavelength of the periodicity was measured by the Fourier analysis of the data. Figure 4 and 5 are the results which indicates that the mean wavelength of the periodic field is 9.65 cm. The strand pitch of the SSC dipole magnet is 86$\pm$5 mm in the inner and 91$\pm$5 mm in the outer coil. A typical measured strand pitch for the same spool of cable are 86 mm and 93 mm. A measurement in magnet DSA320 showed the averaged strand pitch is 88 mm. The wave length is therefore equal or a little larger than the strand pitch of the outer coil. It is definitly larger than the strand pitch of the inner coil cable.

The decay of the amplitude of the periodic field is also analyzed using fourier analysis. Figure 6 shows plots of the field taken after different period of time.

The data are not in the same run but an accumulation of the data taken at different occasion. Therefore, these data may have different offset. Figure 7 is the decay curve of the amplitude obtained from the fourier analysis of these data. It is necessary to accumulate more data to determine the decay behavior but the change in the first 4 hours was very large compared to the change in the next 19 hours.

Discussion

This effect was once interpreted as a result of unequal distribution of strand Ic in the cable. This was a natural thought for HERA magnet because the HERA cable was composed of different batch of strands. However, recent measurement results at BNL and the measurement in this report tells us that the periodic field seems to be a general characteristics of every dipole magnets. The theory based on the inequality of the strands has a difficulty in the coherency between turns. Random coherency between turns could easily average out the periodicity. Since the sextupole contribution is large at $\frac{\pi}{6}$ angle, and there is a region in the magnet where the field never goes up too high hence always leave a large magnetization after a ramp, one could expect a little left over from the averaging out for the sextupole moment[3]. But what we have observed is a dipole component which is most likely averaged out by the phase difference among turns. The rotating coil is also sensitive to the sextupole component but the sensitivety is greatly reduced by the averaging factor $\frac{1}{3}$ and the coil size (quarter inch). Dipole contribution of the magnetization to the field is not as localized as other higher poles. The fact that the phase of the signal did not no change, including when the magnet was ramped up to only 400 A, is also inconsistent with this theory.

One of the possible explanation why the periodicity exists is a formation of eddy current loop chain. Cable is composed of many eddy current loops. The largest loop with longest time constant is the one shown in Fig.8. These loops are tightly coupled with each other by mutual inductances. Therefore, current decrease in one loop makes current increase in other loops. In the case of coupled circuit of two eddy current loop, shown in Fig.9, the relationship between these two currents i_1 and i_2 are:

$$L_1\frac{di_1}{dt} + M\frac{di_2}{dt} + r_1 i_1 = 0 \tag{1}$$

$$L_2\frac{di_2}{dt} + M\frac{di_1}{dt} + r_2 i_2 = 0 \tag{2}$$

The solution of this equation in the form

$$i_{1,2}(t) = Ae^{-\frac{t}{\tau_1}} + Be^{-\frac{t}{\tau_2}} \tag{3}$$

has two time constants. They are

$$\tau_{1,2} = (r_1 L_2 + r_2 L_1) \pm \sqrt{\Delta}$$

where,

$$\Delta = (r_1 L_2 - r_2 L_1)^2 + 4 r_1 r_2 M^2. \tag{4}$$

Short time constant represent the transfer of the current from one loop to another. The main time constant of the decay in the main loop effectively becomes very long. Therefore eddy currents have tendency to be concentrated in one loop in that area. As a result, Eddy current in a cable should look like a chain of loops of strand pitch. Since the loops in other turns are also magnetically coupled, the attractive force between current loops gives loops in each turn a tendency to come to the same position. Therefore the phases of the eddy current loop in every turn becomes the same. Since there are not only two but also many loops coupled together, the behavior of this eddy current is much more complicated. Even the direction of the current could changes at some moment[4]

The time constant of the eddy current can not be as long as the signal we observed. But the periodic field produced by the eddy current makes a periodic pattern of magnetization in the superconductor of the cable. Once the pattern is transfered to the magnetization pattern of the cable, the decay of the pattern shows the same creaping behavior of as the magnetization of the superconductor. If this is the case, the effect will not be related with unequal distribution of Ic nor superconductive splice.

Acknowledgments

We would like to thank M.Warren for his help in the measurement and J.Butteris for making the position sensor.

References

[1]H.Bruck, D.Gall, J.Krzywinski, R.Meinke, H.Preissner, A.Freter, M.Halemeyer, P.Schmuser, R.Steiening, D.terAvest, L.J.M. ban de Klundert, "Observation of a Periodic Fields of the Superconducting HERA Dipole Magnets"-DESY HERA 91-01

[2] M.Wake "Magnetization Effect of Pressure Gage Block", TS-SSC-91-024 Fermilab 1991

[3] M.Kuchnir "Longitudinal Periodicity in Superconducting Dipole Magnets" Fermilab TM-1712

[4] B.Turck "Influence of a transverse conductance on Current Sharing in a two-layer Superconducting Cable",Cryogenics 14 448 (1974)

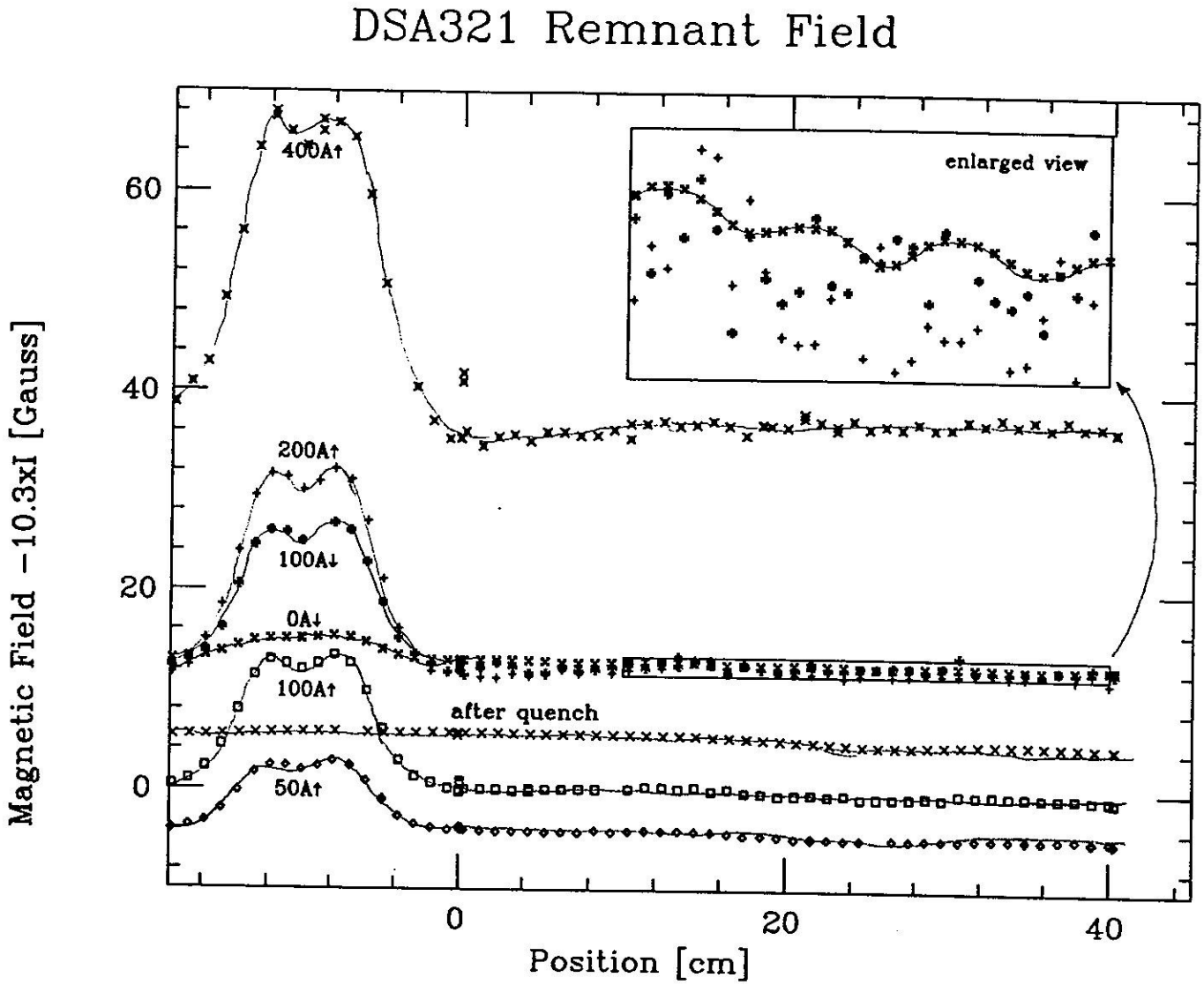
DSA321 Remnant Field
400A↑
200A↑
100A↓
0A↓
100A↑
after quench
50A↑
enlarged view
Magnetic Field −10.3xI [Gauss]
Position [cm]
60
40
20
0
0
20
40

Fig 7

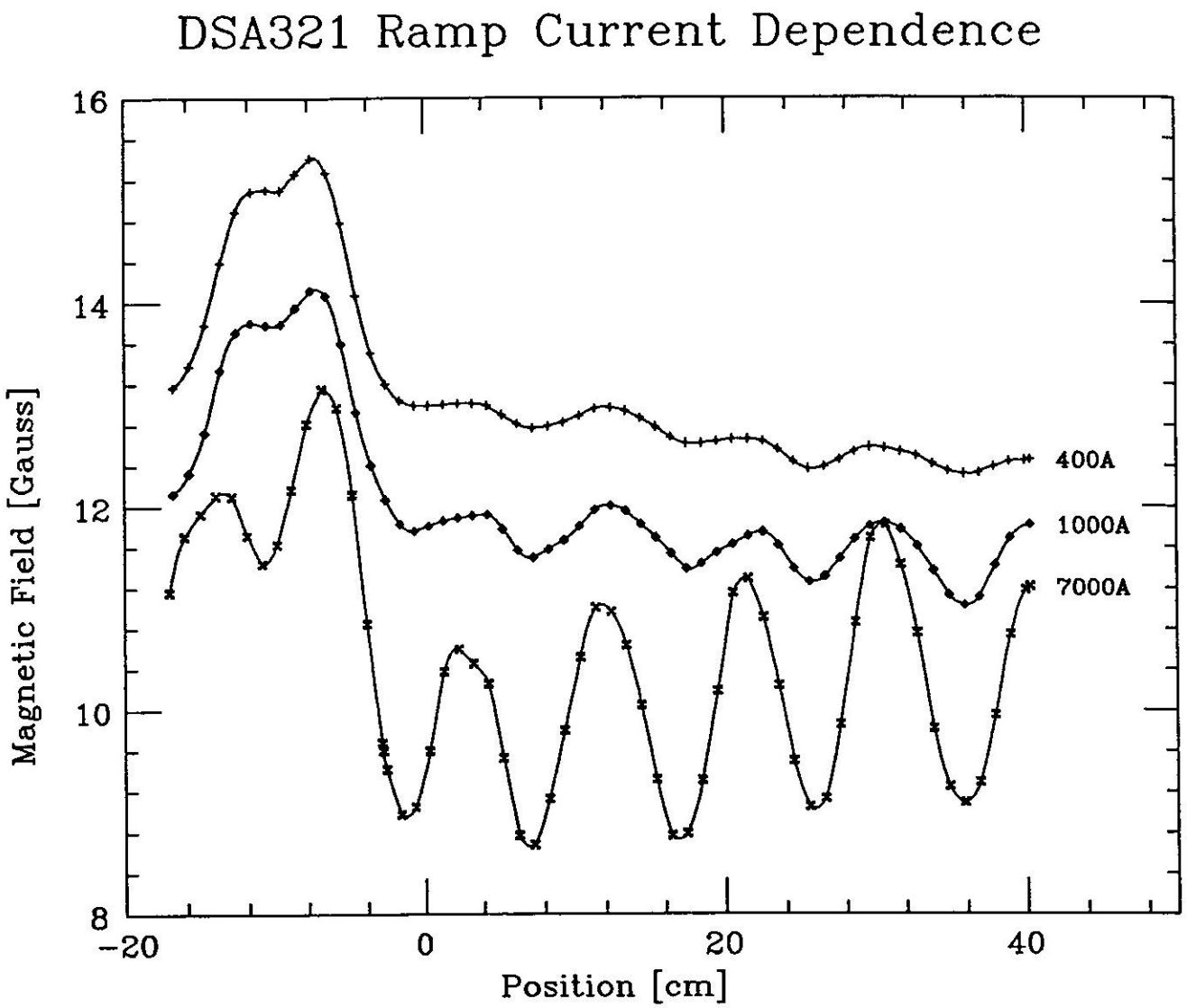
DSA321 Ramp Current Dependence
16
14
12
10
8
Magnetic Field [Gauss]
-20
0
20
40
Position [cm]
400A
1000A
7000A

Fig 2

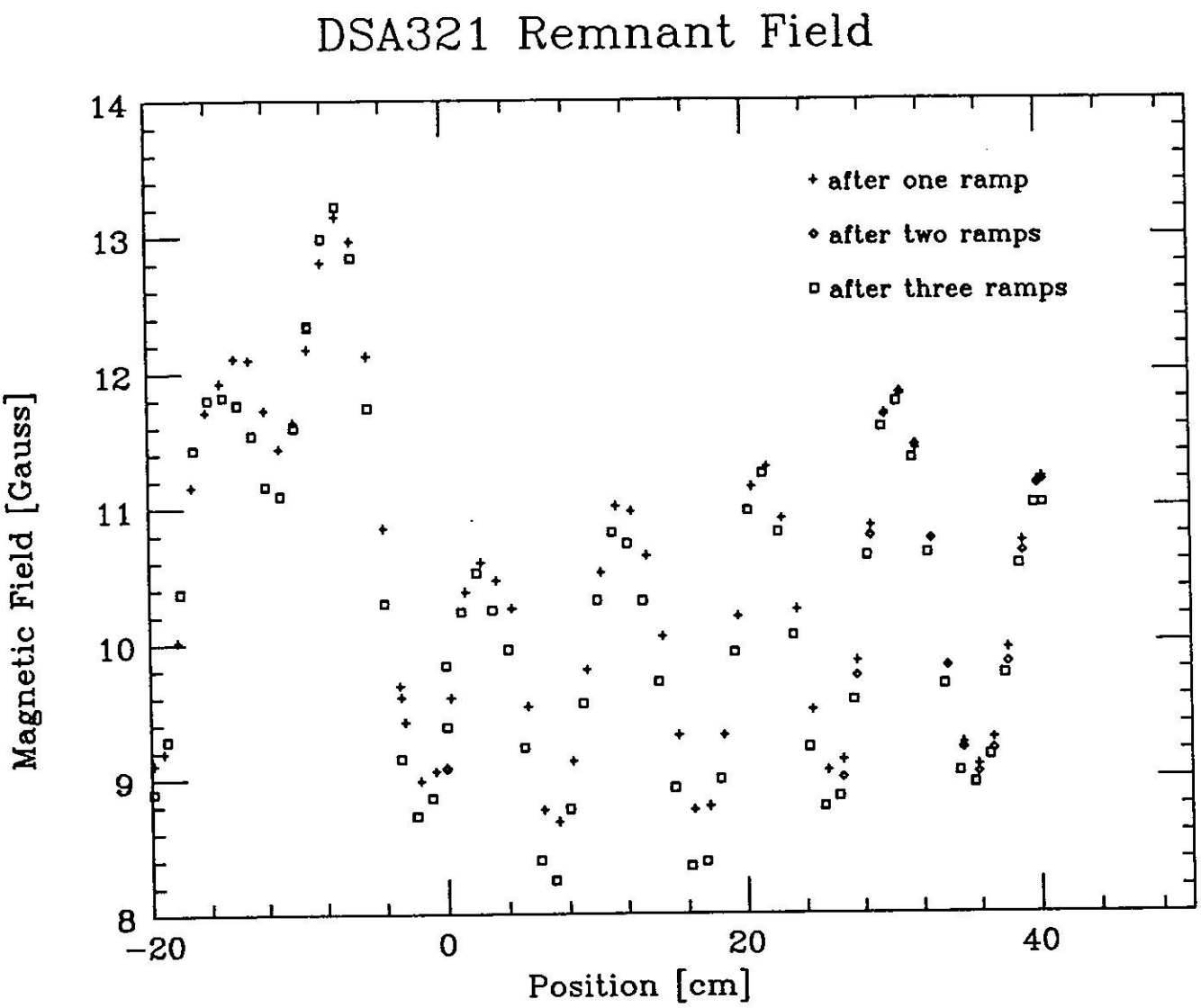
DSA321 Remnant Field
after one ramp
after two ramps
after three ramps
Magnetic Field [Gauss]
Position [cm]
14
13
12
11
10
9
8
−20
0
20
40

Fig 3

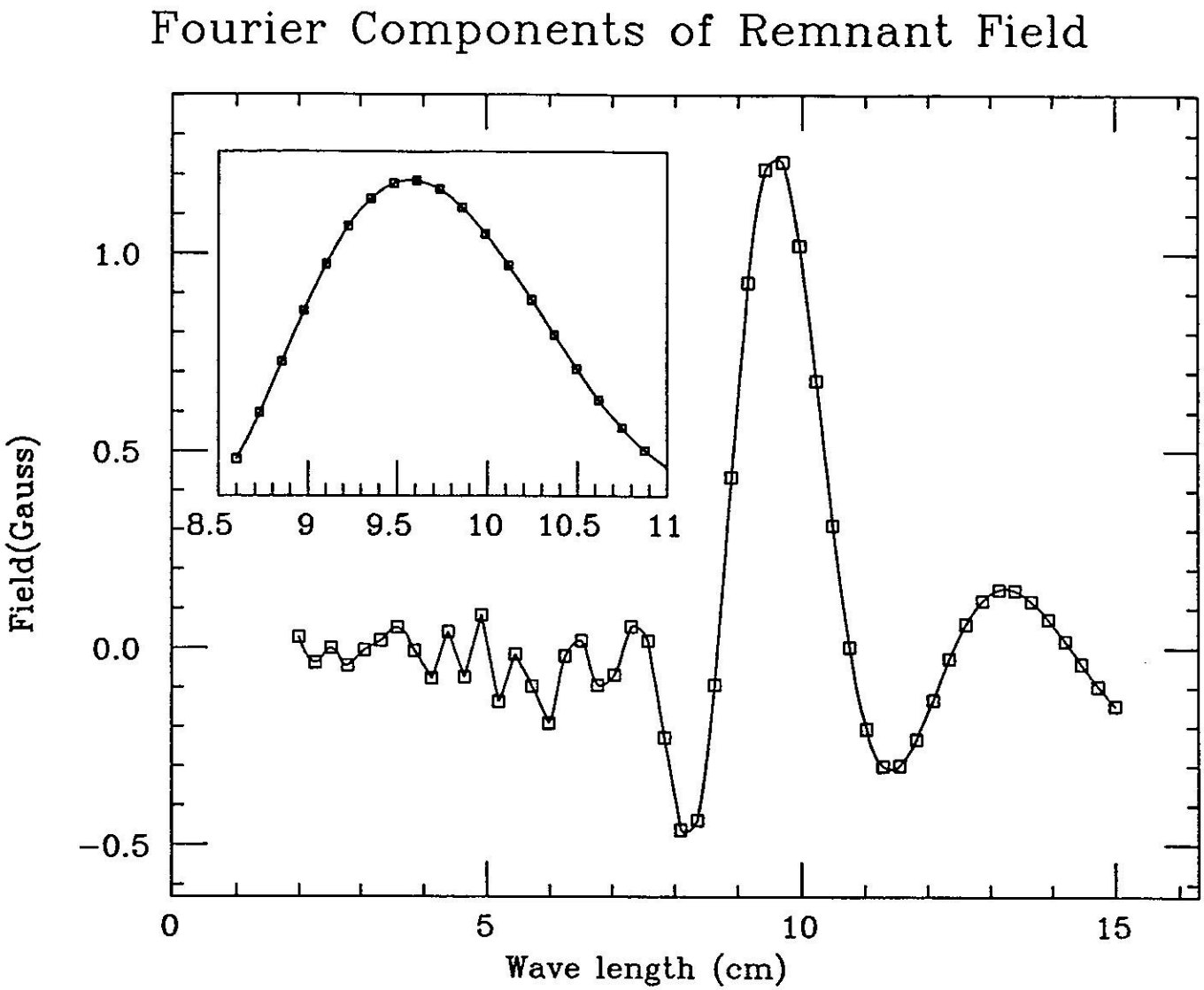
Fourier Components of Remnant Field
Field(Gauss)
1.0
0.5
0.0
−0.5
0
5
10
15
Wave length (cm)
8.5
9
9.5
10
10.5
11

Fig 4, 5

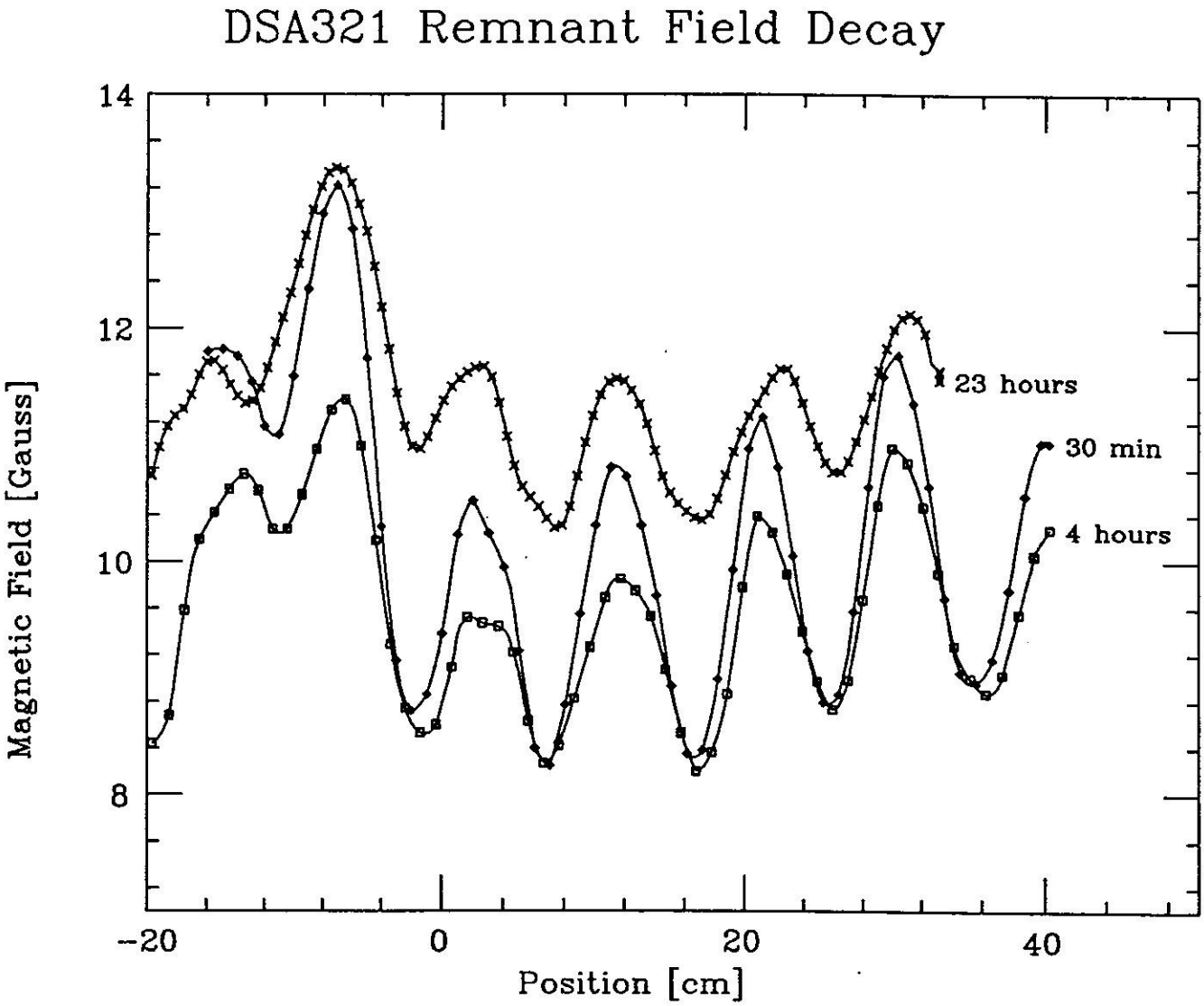
DSA321 Remnant Field Decay
14
12
10
8
Magnetic Field [Gauss]
-20
0
20
40
Position [cm]
23 hours
30 min
4 hours

Fig 6

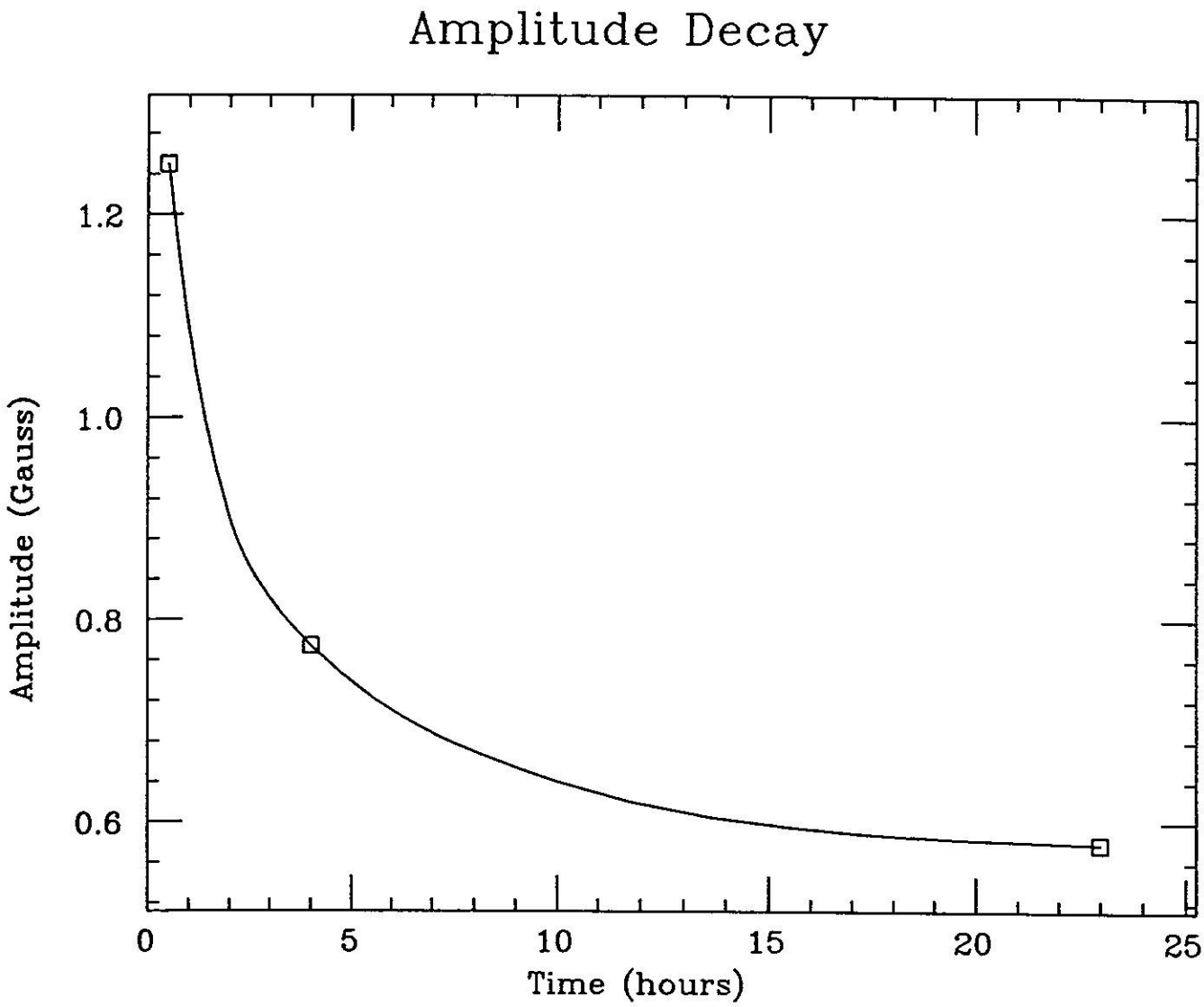
Amplitude Decay
Amplitude (Gauss)
1.2
1.0
0.8
0.6
0
5
10
15
20
25
Time (hours)

Fig. 7

Fig.9

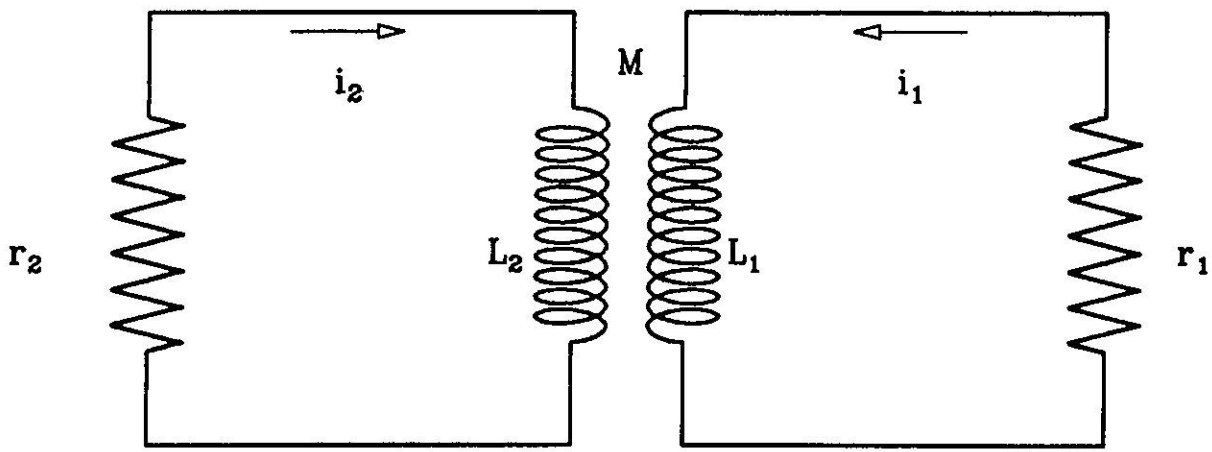

Fig. 8

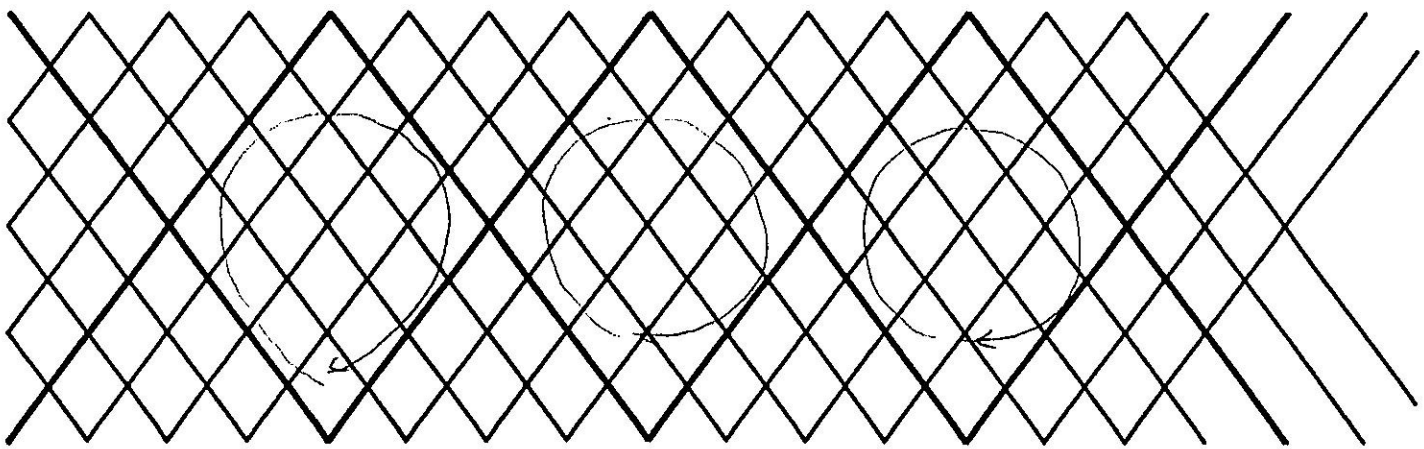

Distribution:

FNAL
- S. Delchamps
- S. Gourlay
- R. Hanft
- T. Jaffery
- W. Koska
- M. Kuchnir
- M. Lamm
- P. Mantsch
- P. Mazur
- G. Pewitt
- J. Strait
- M. Wake

BNL
- W. B. Sampson

DESY
- P. Schmuser

SSCL
- A. Devred
- R. Schermer
- R. Stiening

```
-------------------------------
r_nominal          =   2.183 inches
rv                 = -12.000 mils
rh                 =   6.000 mils
skin_stress_300K   =  25.000 kpsi
skin_stress        =  45.000 kpsi
contract_collar    =  -0.003
contract_yoke      =  -0.002
-------------------------------
```

							T = 300 K				T = 4 K							
drv/drh	drv/dpr	drh/dpr	prestr	dcool	dh/ds1	dh/ds2	rh	rv	rv_rh0	sk_rh0	rh	rv	rh_rv0	rv_rh0	rh_sk	rv_sk	sk_rv0	sk_rh0
-0.54	0.56	-0.05	10.00	-2.25	-0.25	-0.03	5.5	-6.4	-3.4	22.3	3.4	-9.8	-14.8	-8.0	0.0	-8.0	-	14.
----- Vary Coil Prestress and Cooldown Loss -----																		
-0.54	0.56	-0.05	13.00	-2.25	-0.25	-0.03	5.3	-4.7	-1.8	21.7	3.3	-8.2	-11.8	-6.4	0.0	-6.4	-	13.
-0.54	0.56	-0.05	7.00	-2.25	-0.25	-0.03	5.6	-8.1	-5.0	22.9	3.6	-11.5	-17.8	-9.6	0.0	-9.6	-	15.
-0.54	0.56	-0.05	10.00	-3.25	-0.25	-0.03	5.5	-6.4	-3.4	22.3	3.5	-10.4	-15.8	-8.5	0.0	-8.5	-	14.
----- Vary dr/d(prestress) -----																		
-0.54	0.44	-0.05	10.00	-2.25	-0.25	-0.03	5.5	-7.6	-4.6	22.3	3.4	-10.8	-16.5	-8.9	0.0	-8.9	-	14.
-0.54	0.56	0.00	10.00	-2.25	-0.25	-0.03	6.0	-6.4	-3.2	24.4	3.8	-9.8	-14.4	-7.8	0.0	-7.8	-	16.
----- Choose values that give a small collared coil -----																		
-0.54	0.44	-0.05	7.00	-3.25	-0.25	-0.03	5.6	-8.9	-5.9	22.9	3.6	-12.5	-19.6	-10.6	0.0	-10.6	-	15.
----- Vary dr/d(skin stress) -----																		
-0.54	0.56	-0.05	10.00	-2.25	-0.32	-0.03	5.5	-6.4	-3.4	17.2	3.4	-9.8	-14.8	-8.0	0.0	-8.0	-	11.
-0.54	0.56	-0.05	10.00	-2.25	-0.25	-0.05	5.5	-6.4	-3.4	22.3	3.4	-9.8	-14.8	-8.0	0.0	-8.0	-	14.
-0.54	0.56	-0.05	10.00	-2.25	-0.32	-0.05	5.5	-6.4	-3.4	17.2	3.4	-9.8	-14.8	-8.0	0.0	-8.0	-	11.
----- Vary drv/drh -----																		
-0.46	0.56	-0.05	10.00	-2.25	-0.25	-0.03	5.5	-6.4	-3.9	22.3	3.4	-9.8	-18.0	-8.3	0.0	-8.3	-	14.
-0.64	0.56	-0.05	10.00	-2.25	-0.25	-0.03	5.5	-6.4	-2.9	22.3	3.4	-9.8	-12.0	-7.7	0.0	-7.7	-	14.